prepared for the
National Institutes of Health
National Institute of Neurological Disorders and Stroke
Neural Prosthesis Program
Bethesda, Maryland 20892

ELECTRODES FOR FUNCTIONAL ELECTRICAL STIMULATION

Contract #NO1-NS-6-2346

Progress Report #7
July 1, 1998 - September 30, 1998

Principal Investigator
J. Thomas Mortimer, Ph.D.

Applied Neural Control Laboratory
Department of Biomedical Engineering
Case Western Reserve University
Cleveland, OH USA

TABLE OF CONTENTS

SECTION B. DESIGN AND FABRICATION OF ELECTRODES, LEADS AND CONNECTORS

B.2.1.2: Polymer-Metal Foil-Polymer (PMP) Cuff Electrodes

The polymer-metal foil-polymer (PMP) electrode is a novel design that attempts to improve the mechanical reliability and ease the manufacturing process of spiral nerve cuff electrodes. The electrode design uses laser machining technology to fabricate an electrode pattern in a polymer-metal foil laminate. During this reporting period, we began work on a third version of the electrode pattern.

Previous Work

Work was done in Period 6 to correct the excess expansion, which was occurring at the sites where isolation cuts had been made, during the stretch lamination procedure in Step 5 of the fabrication process. Our efforts were directed at finding a way to ensure proper distribution of the elastomer prior to applying the 2 ton load in the press. In addition to the new distribution method, we decided to switch to an elastomer, MED-6015, which has a much lower viscosity and facilitates elastomer flow during the lamination process. A new stretch formula was determined for the cuffs being developed using a 2 mil sheet as the stretched layer.

Current Work

In Period 7, the PMP2 electrodes were furthered through the fabrication process. The new 2 mil stretch formula was used for the cuff lamination. A picture of a 3.0mm PMP2 cuff electrode after Step 5 of the fabrication process is shown below.

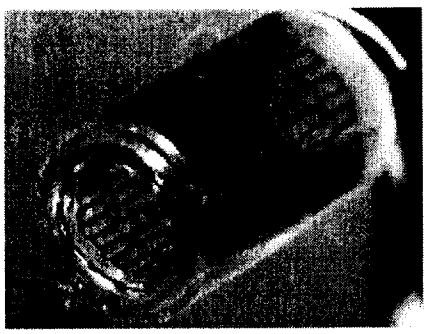

Figure B.1: The picture above is of a 3.0mm PMP2 cuff electrode after Step 5 of the fabrication process.

After the stretch lamination had been completed, the PMP2 electrodes were unwrapped and placed back in the laser machining frames. It was difficult to clamp the electrodes properly in the frame since the electrode had already been cut into its final desired shape. This will be rectified in the future by not cutting out the electrode cuff until after Step 6, the laser machining of the stimulation sites, has taken place. Despite the difficulties experienced with holding the curled structure flat, the stimulation site pads were removed by the laser with satisfactory results.

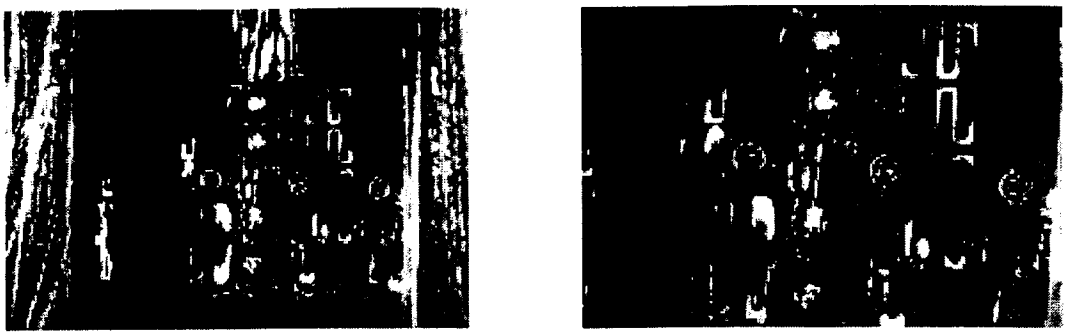

Figure B.2: The pictures above show the electrodes after the stimulation sites had been opened. The picture on the left is of an electrode in the laser machining frame. The electrodes were difficult to clamp in the frame since the silicone cuff was cut very close to one edge of the electrode. The picture on the right is a closer view of the stimulation sites. Odd lighting is a result of the inability to hold the cuff structure flat.

The completed PMP2 electrodes were then cleaned and sterilized for implant. Each electrode was labeled and all of its fabrication details can be found in separate electrode tracking reports kept in the laboratory.

To address the excess expansion problems experienced with the PMP2 electrodes, a new conductivity cut pattern was created which had fewer isolation cuts. The new AutoCAD file is shown below. Cuts were placed in such a way to avoid having the holes close together.

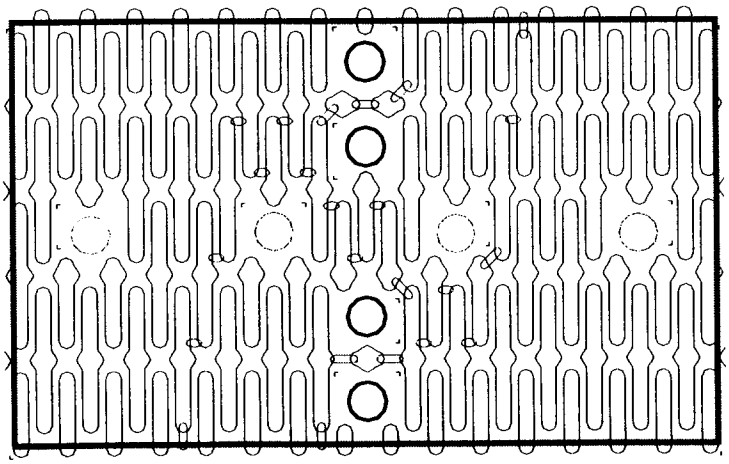

Figure B.3: AutoCAD file showing the new cut pattern to isolate the conductivity paths. The new pattern of cuts are the ovals and ellipses shown on the basic structure of the electrode. These laser cuts are made during Step 3 of the fabrication process.

In addition to the new laser pattern, we used a 3 mil sheet of silicone for the stretch sheet. It is thought that the thicker sheet will take the desired cuff shape with less stress applied to the electrode structure. Because of the switch to the 3 mil sheeting, new experiments were

performed to determine the amount of stretch needed to achieve a desired diameter. It was found that the 3 mil sheet of MED-4550 with the MED-6015 elastomer needs to be stretched 1.5 times the stretch calculated from the original formula.

Two new electrodes were attempted using the 3 mil stretch sheet and the new laser cut file. These electrodes are termed PMP3 due to the slight design change. Steps 1 and 2 of the fabrication process were completed in the same manner as in the PMP2 electrode.

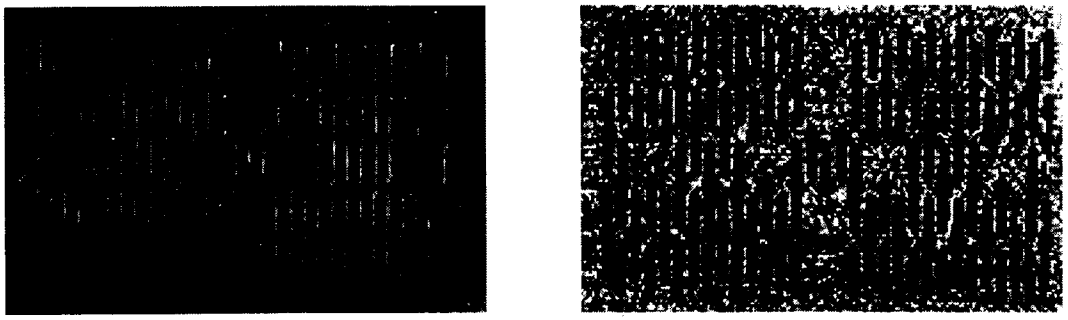

Figure B.4: The picture on the left is of a 3.0mm electrode after the first laser pass. The picture on the left was taken of the same electrode after Step 2, the lamination of the platinum.

Step 3 was completed on both electrodes using the new laser cut pattern for the conductivity path isolation. It can be seen from the pictures below that some of the cuts appear to still contain platinum and are therefore incomplete. There are also a few places where the silicone was torn away from the platinum near the cuts.

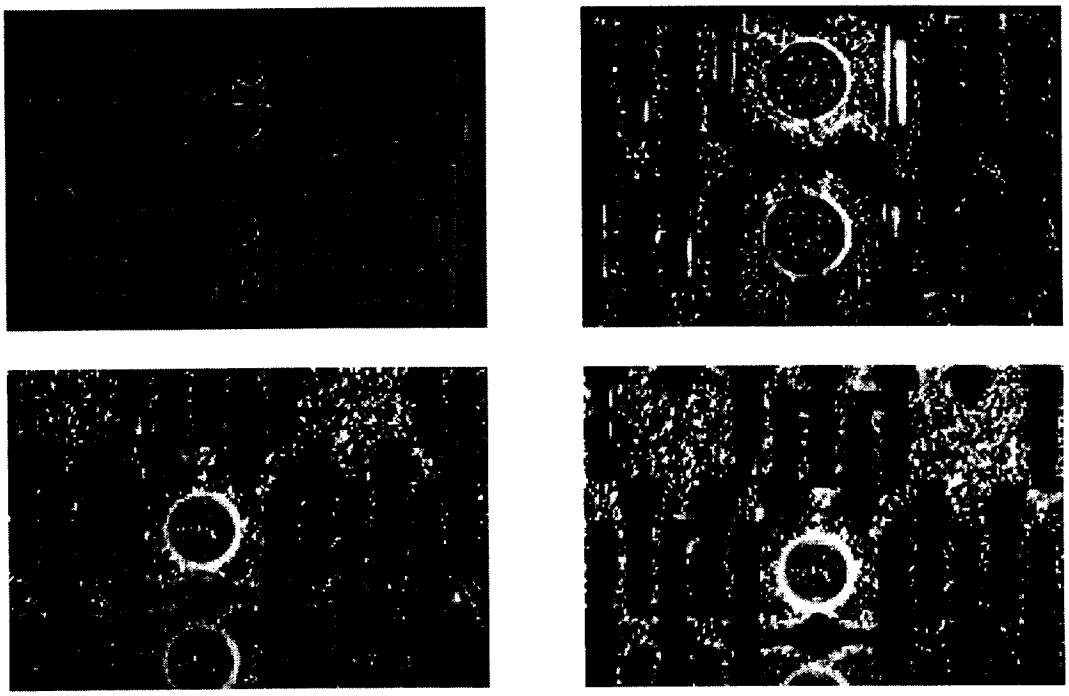

Figure B.5: The pictures shown above are of the 3.0mm electrodes after Step 3 of the fabrication process. It can be seen in the higher magnification pictures that the cuts to isolate the conductivity paths do not look complete. There is also some tearing of the silicone and, in some places, removal of the silicone next to the cuts.

It was determined that the incomplete cutting of the conductivity isolation was due to the recent material changes made in the electrode components. Samples were made using this new make-up and it was found that more laser pulses were needed to properly cut the silicone. In the future, any change in materials will be accompanied by laser trials.

Future Work

The PMP3 electrodes will be furthered through the fabrication process in Period 8. A new batch of 10 PMP3 electrodes will also be fabricated for implant and testing barring any problems with the current PMP3 electrodes. An evaluation of the new MED-6015 elastomer will also take place. This is because it has been observed that the new elastomer has a tendency to cause wrinkles in the cuff and may have a relaxing, or inhibiting, effect on the curl of the cuff. Comparisons will be drawn between samples made with the old MED-4211 elastomer and the new MED-6015 elastomer. New elastomers may be researched as well.

B.2.4.1: Silicone Rubber Sheeting

The goal of this project was to establish performance specifications for the silicone rubber sheeting used in the spiral cuff electrode fabrication. Tests were conducted to determine the mechanical and physical properties of four different silicone rubber sheeting formulations. Additionally, we investigated the effects of aging and sterilization on these properties. All specimens tested had a thickness of 0.002inch (50μm). The control sample was supplied by

Dow Corning and manufactured by AVECOR (Q7-4550.) This sheeting was used in the manufacture of our previous cuffs, but can no longer be used since it is not approved for long-term human implants. The new formulations are MED-4550, MED2-6640, and MED2-6641-1 and are supplied by NuSil and manufactured by Specialty Silicone Fabricators.

Current Work

In this period, we measured the contact angle, coefficient of friction, and tensile strength. Visual imperfections, such as tears, or unusual markings on the samples were noted. A few of the samples were noted to have small tears along the edges within the gage length. These tears were thought to have been incurred during the cutting of the samples. However, the tears did not seem to have been the cause of the breaks during the tensile testing. It was also observed that each silicone sheeting formulation had its own imperfections due to the manufacturing. For example, it was noted that all the MED-4550 samples had small bumps throughout the entire material and the MED2-6640 samples had small light horizontal lines running throughout. These visual properties had no noticeable effect on the results of the testing.

The dynamic contact angle was measured using a contact angle goniometer. A microsyringe attached to this device released a small drop of ultrapure water on to the surface of a silicone rubber sheeting sample, and the angle of the water droplet was measured. Another drop was then added on top of the first and the angle was measured again. This procedure was repeated until about 5 or 6 advancing angles were measured. The receding angles were measured by successively removing tiny drops with the microsyringe. The larger the advancing angle, the more hydrophobic a material is. The smaller the advancing angle, the more hydrophilic a material is. Hydrophobic materials are non-polar and cells do not adhere as well to these materials as they do to the polar, hydrophilic, materials. For our application, a very hydrophilic material is desired to since it is thought that a hydrophilic material will reduce the force it takes to expand the cuff. Analysis of these angle measurements explains the surface properties. A large standard deviation (greater than 2°) in either the advancing or the receding angle is interpreted to mean that there is a rearrangement of the hydrophilic groups on the surface of the sheeting. A hydrophilic rearrangement also occurs if the average receding angle differs from the average advancing angle by a large amount.

The advancing angles for each formulation of sheeting were averaged and are presented below by comparison of the sheeting formulations for the control, aged, and sterilized groups.

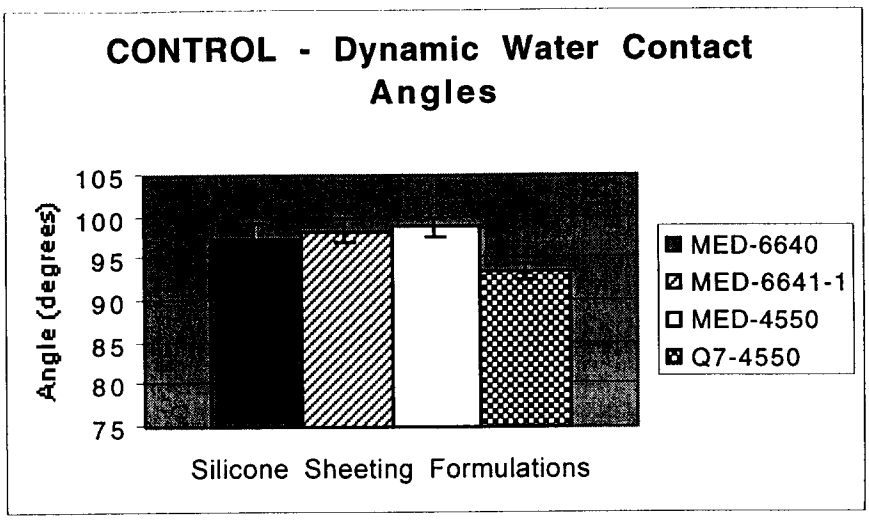

Figure B.6: The bar chart above represents the averages of the advancing angles for the 4 silicone sheeting formulations tested. Specifically, these samples were in the control group.

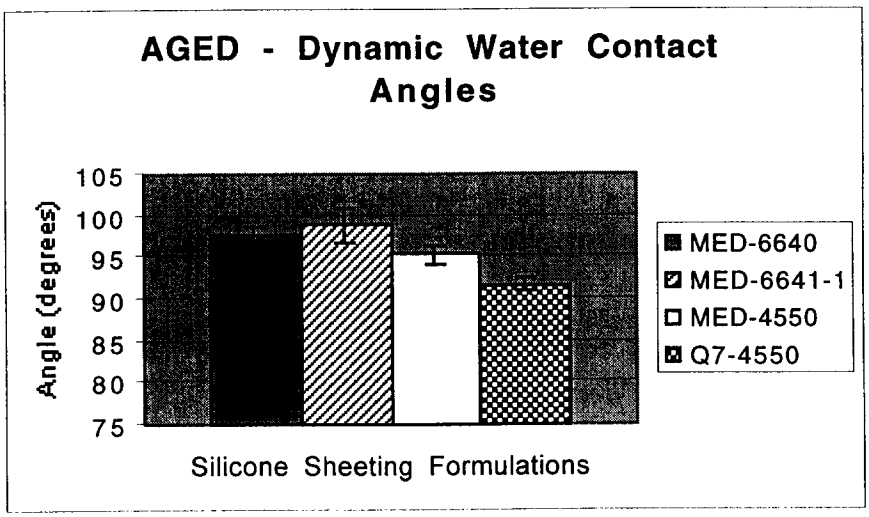

Figure B.7: This bar chart represents the averages of the advancing angles of the 4 different sheeting formulations tested. The samples used in this chart were aged.

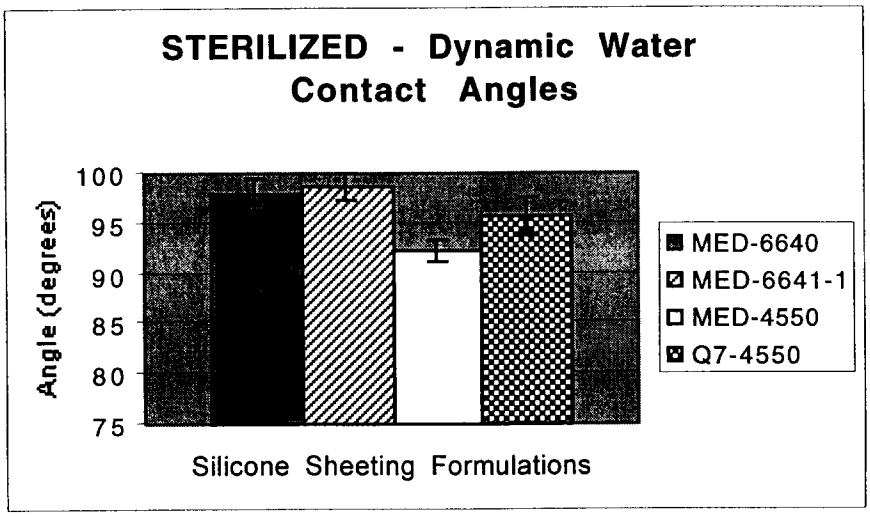

Figure B.8: This bar chart represents the averages of the advancing angles of the 4 different sheeting formulations tested. The samples used in this chart were sterilized.

The MED2-6641-1 consistently has the highest advancing angle for each group, which means that it is the most hydrophobic of the formulations. The MED-4550 is a replication of the Q7-4550 formulation, so it was expected that these formulations would have similar properties. Instead, the MED-4550 actually becomes more hydrophilic with aging and sterilization. The Q7-4550 was, on average, the most hydrophilic of the formulations tested.

Some errors could have occurred during the testing of these samples. Namely, if the samples were not completely flat, it could have caused a large deviation between angle measurements. In addition, improper calibration of the instruments could have skewed groups of measurements. Lastly, the age of the sheeting may have affected the results. Specifically, the Q7-4550 formulation tested was approximately 5 years old while the remaining formulations were a year or less old.

The coefficient of friction of the samples was measured using an ASTM approved coefficient of friction fixture as described in PR #6. These measurements were taken using a crosshead speed of 200mm/min. The load cell was set on the lowest available setting, which yielded a ±1N error. This error is large for our application and its affect will be revealed in the standard deviations of the measurements. However, useful comparisons can still be made between the coefficients of friction for each formulation. The data for this test is still being reduced and analyzed. The results of this process will be presented in PR#8.

Once the observations, contact angle, and coefficient of friction measurements were completed the samples were tensile tested to failure. This was done by gluing the ends of the samples to aluminum tabs using MED-1137 silicone adhesive. The tabs could then be properly gripped by the tensile tester and pulled until the sample broke. The results of each test were graphed and the information regarding the percent elongation and maximum load of the samples were extracted for use in our evaluation. The percent elongation relates to the distance that the

silicone can be elastically stretched before failure. The percent elongation data for the samples is represented by the bar charts below.

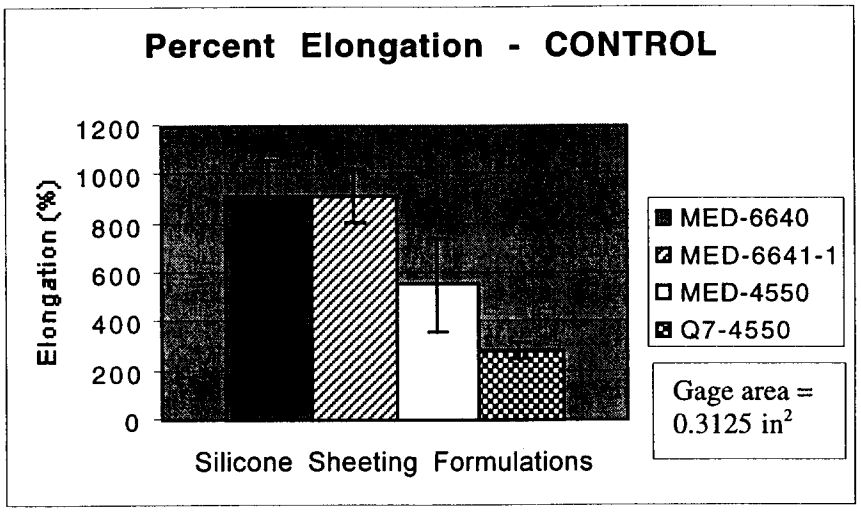

Figure B.12: The bar chart above represents the amount that each formulation will elongate before failure. This elongation is shown as a percentage of its original gage length. The data above is for the control groups.

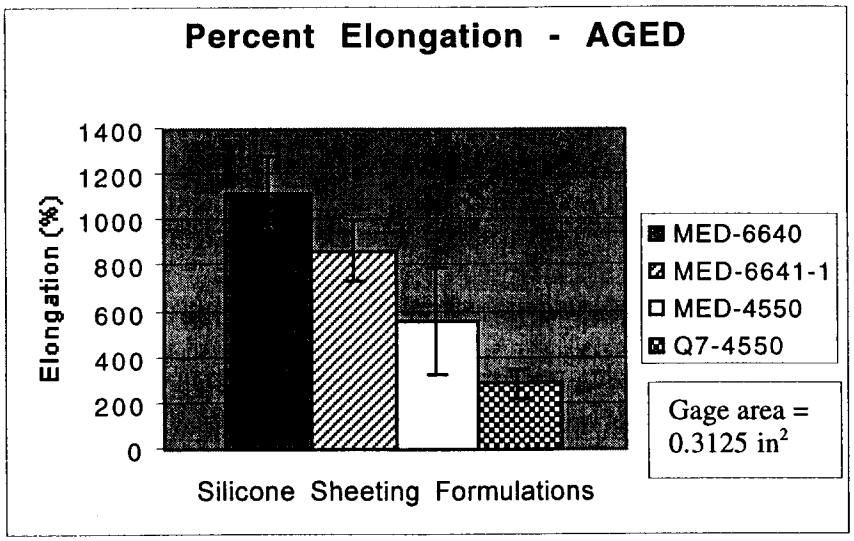

Figure B.13: The bar chart above represents the amount that each formulation will elongate before failure. This elongation is shown as a percentage of its original gage length. The data above is for the aged groups.

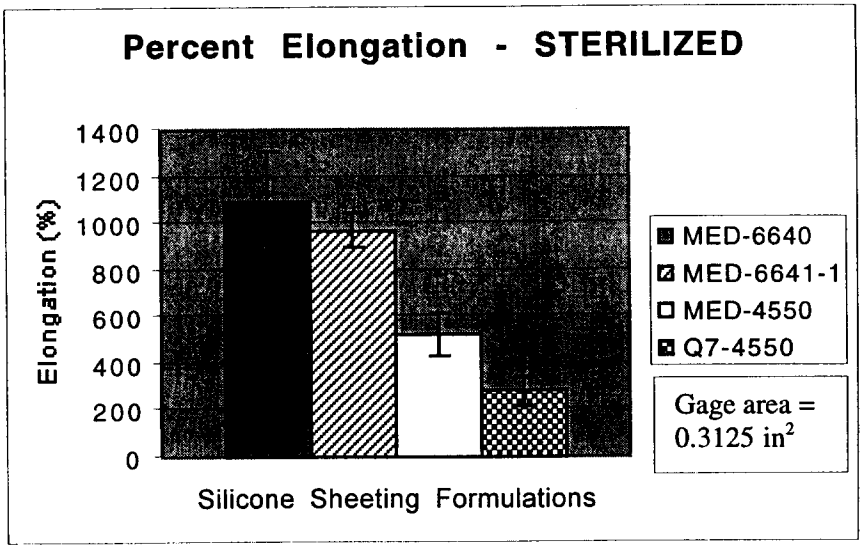

Figure B.14: The bar chart above represents the amount that each formulation will elongate before failure. This elongation is shown as a percentage of its original gage length. The data above is for the sterilized groups.

Comparison of the above data with manufacturer specifications reveals similar results. MED2-6640 is specified by the manufacturer as having, on average, 1100% elongation. Our data shows MED2-6640 as having an 1100% elongation. MED-4550 and Q7-4550 are both supposed to have a minimum of 500%, and an average of 600%, elongation. The MED-4550 falls within the manufacturer certified range, but the Q7-4550 falls well below at 300% elongation. This is most likely because the Q7-4550 was at least 3 years old. Manufacturer specifications for MED2-6641-1 were not available. The charts also reveal that aging and sterilization actually increases the elongation of the materials. This could be caused by a relaxation of the silicone and, although this should have no effect on our application, it may be important in later designs. The charts also reveal large differences in elongation between the formulations tested. This property may be important when choosing a silicone that will perform to a desired specification when stretched.

The maximum load taken by the samples before failure was also recorded. Bar charts representing this property are contained below.

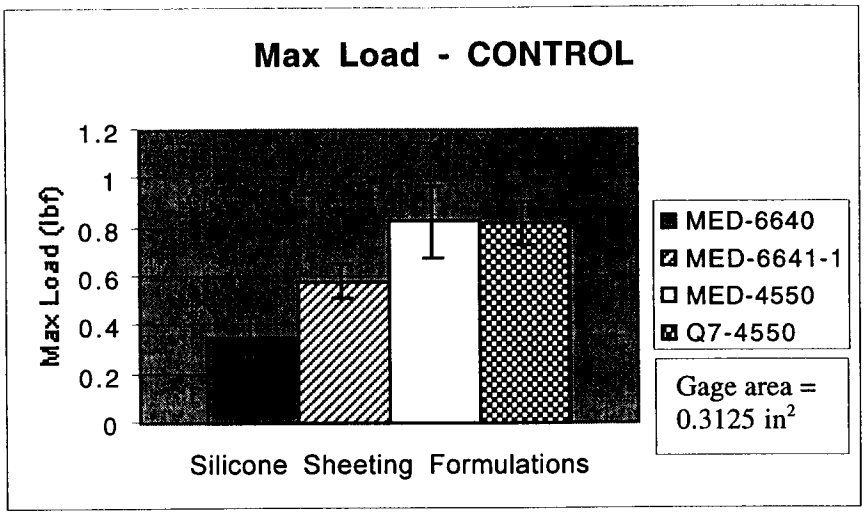

Figure B.15: The maximum loads that the silicone sheeting samples were able to withstand before failure are presented in the bar chart above. This bar chart contains the data for the control groups.

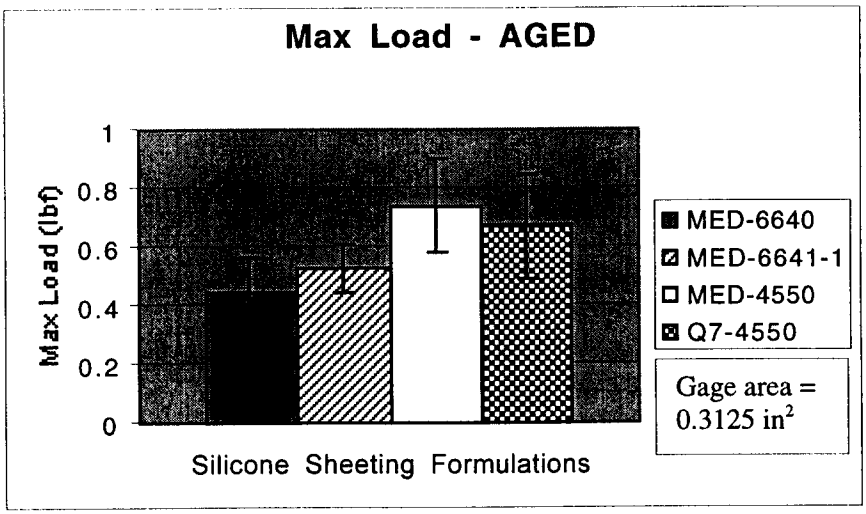

Figure B.16: The maximum loads that the silicone sheeting samples were able to withstand before failure are presented in the bar chart above. This bar chart contains the data for the aged groups.

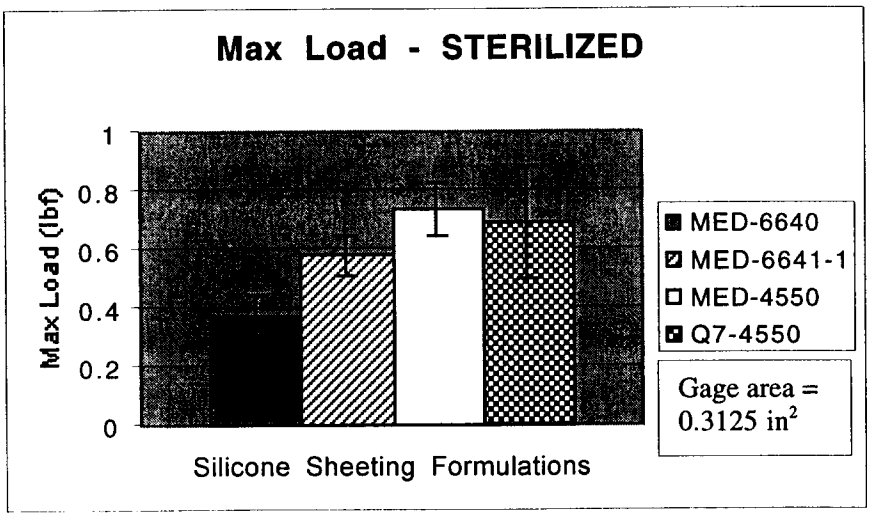

Figure B.17: The maximum loads that the silicone sheeting samples were able to withstand before failure are presented in the bar chart above. This bar chart contains the data for the sterilized groups.

It can be seen from the maximum load data that the loads decrease only slightly when the materials are aged and sterilized. When comparing the charts for the percent elongation and those for the maximum load, it can be seen that the materials react in the reverse manner between the elongation and the load. Those materials that have a very high percent elongation consequently have a very low maximum load. Specifically, MED2-6640 and MED2-6641-1 had high percent elongation's, while MED-4550 and Q7-4550 and the highest maximum loads. It is important to find a material that has a balance of these two properties.

One of the factors that could have caused error in the tensile tests was that at times the silicone adhesive was pulled away from the tab and added to the load needed to break the samples. For this reason, the elongation's and maximum loads may be slightly higher than actual. Improper positioning and gluing of the silicone on the aluminum tabs may have also added to the deviation by causing the silicone to break on the outskirts of the gage length.

Future Work

The data presented in this report will continue to be reduced and analyzed in order to determine specifications for silicone rubber sheeting. These specifications and the coefficient of friction data will be presented in PR#8. Throughout the rest of the contract, different silicone sheeting formulations will continue to be studied. Others may be tested and will be compared to this base of data. Should our application change in any way, this data will be revisited to ensure that the sheeting used is the proper material for the application.

B.2.4.4 Mechanical Failure Mode of Completed Electrodes

In the contract, we proposed tensile testing the completed electrode to failure with axial tension. It has since been decided that this is not a realistic form of failure for the spiral cuff electrode. The electrode does not undergo excessive axial tension, and if at any point it did, it is believed that the nerve would be damaged much earlier than the cuff would fail. The likely

failure due to tension would be the breakage of the lead or weld due to tethering of the leads. This form of failure was tested with the weld strength testing performed and reported in Period 6. The tensile testing of the electrode will therefore not be performed at this time.

B.2.5.1 Flexion Testing

In the contract, we proposed a flexion test that would piston the electrode up and down using a localized force for 5 million cycles. Although an *in vivo* electrode might undergo some point flexion due to nearby muscle flexion, the flexion would most likely be a distributed pressure on the nerve and electrode. The proposed test would therefore not be a reasonable mode of failure. The 5 million cycles would also be excessive considering what the electrode would undergo. It has been decided that this test will not be performed in lieu of two new tests that will better represent the actions with which the cuff will be exposed.

One of the tests to be performed will be a rolling test. The spiral cuff will be opened and held flat several times during the fabrication and cleaning processes. The cuff will also be opened during implant. To evaluate this process, 5 electrodes will be unrolled 100 times and the conductivity of each electrode will be checked every 10 cycles. A cuff will realistically not be opened more than 10 times, therefore 100 cycles was chosen to give the test a safety factor of 10.

The second flexion test to be performed will involve the study of the electrode lamination after being aged *in vitro.* It is has been reported that the absorption of lipids could cause degradation of the silicone rubber. It is also thought that when the lipids are combined with flexion, this causes a significant decrease in the mechanical properties of the silicone. Five electrodes, and their surrounding pieces of silicone rubber from manufacture, will be continuously flexed while being aged *in vitro.* The samples will be placed in a simulated extracellular fluid at an elevated temperature to accelerate the aging process. Specifically, they will be tested for 30 days in a bath held at 85°C. At test completion, the five electrodes will be studied for delamination. The color of the silicone rubber pieces will be observed and the pieces will be tensile tested to failure to observe any changes in their mechanical properties.

B.2.6 *In Vivo* Testing

We proposed in the contract that FWF and PMP electrodes be implanted in the right hind limb of cats with stimulation for electrode reliability. After 6 months, the encapsulation tissue would be excised and the electrodes would be evaluated. We now propose some changes in the original format. The FWF electrodes were based on a serpentine design, which had a 1 mm pitch. This design yielded a curl that visually appeared to be stiffer than electrodes previously developed. Production was therefore continued with only the PMP electrodes, which produce a smoother curl due to the reduction in the pitch to 0.3 mm. The PMP electrodes that will be evaluated will be implanted and stimulated according to the protocol in part C of the contract. These electrodes will be PMP electrodes implanted for 3-month periods. We were not aware of any advantages to implanting different cats for part C and for this *in vivo* test simultaneously. We feel that the same results can be achieved by using the electrodes implanted in part C. The encapsulation tissue will still be excised and preserved in fixative and the electrode will undergo the same evaluation as was previously proposed in the contract. Implants have already begun, and results are expected in the last few periods of the contract.

SECTION C. IN VIVO EVALUATION OF ELECTRODES

C.I.2.2: Selective Activation Stability Over Range and Time; Chronic Animal Tests

Abstract

The objective of this project is to qualify nerve cuff electrodes for use in human subjects. We have two designs that we believe are or will be technologically feasible and reliable, the PMP design and the wiggle-wire design. The first design, the PMP electrode, contains a sheet of platinum that is cut with a laser and embedded into the silicone rubber to produce a thin, multi-contact nerve cuff electrode. The wiggle-wire electrode is produced with the lead wires being bent back and forth in the plane of the electrode to allow the conductor to accommodate compression and tension when the cuff is opened and closed.

Chronic experiments, designed to provide both histological data on the safety of these electrode designs and stimulation results on the long-term stability of the recruitment properties of the electrodes, were begun. We believe that in the chronic preparation, where the cuff electrode is stabilized with connective tissue, we can test additional techniques in an attempt to achieve sub-fascicular selectivity. The stability of the electrode was previously tested by Grill [1996] based on the change in the threshold value over time but the stability of more complicated electrode configurations were not tested. During the course of these experiments, we will test field steering techniques to verify that their properties stabilize over time.

Progress

Five implantation procedures were performed of which 2 were performed at the closing of the previous reporting period. In one case, the animal did not survive the surgery. We believe that reactions with the anesthesia were a major factor for this outcome. Of the remaining four animals, two animals were implanted with a wiggle-wire type four contact nerve cuff electrode and two animals were implanted with a PMP type four contact nerve cuff electrode. In each animal, the electrodes were implanted and the animal was monitored for any unusual pain, loss of function or loss of reflex. No significant change in animal behavior, reflexes or strength was found in any of the animals. Testing of the torque responses due to stimulation applied to the nerve cuff electrode began approximately three weeks post-implant. A three-week time was decided based on previous studies that showed full encapsulation and stabilization of the nerve cuff electrode took place over the first three weeks. Approximately three and a half weeks post-implant (a few days after the first test), one of the animals showed signs of deteriorated skin along the middle and lower back. The source of the skin deterioration is not known but suspected to be due to a loss of blood supply. One possible mechanism by which accidental disruption of the blood supply may have occurred was through the subcutaneous tunneling of the lead wires up the back. Due to the skin condition, the animal had to be euthanized at seven weeks. A perfusion procedure was performed to fix the nerve and surrounding tissue for histology. Both the region surrounding the sciatic nerve at the level in which the nerve cuff was implanted and the regions around the lead wire were taken for future histological processing.

The processing of data from the animal that was terminated at seven weeks was begun. Figures C.1-C.4 display the results over four different testing sessions performed over three different days. Two test sessions were performed on the same day. Prior to conducting the second test on the same day, the animal was removed and then re-mounted in the recording apparatus. This removal was carried out to study the variability introduced by inaccuracies in the alignment of the limb within the recording apparatus. In Figure C.1 are the data from stimulation applied to the 0° position contact. Five of the six recruitment curves produced medial rotation before plantar flexion. Only the torque trace produce on the first experimental day resulted in output torque that did not produce medial rotation before plantar flexion. In each case, the maximum amount of medial rotation produced in a particular torque trace was indicated by an arrow labeled with a letter corresponding to the figure legend.

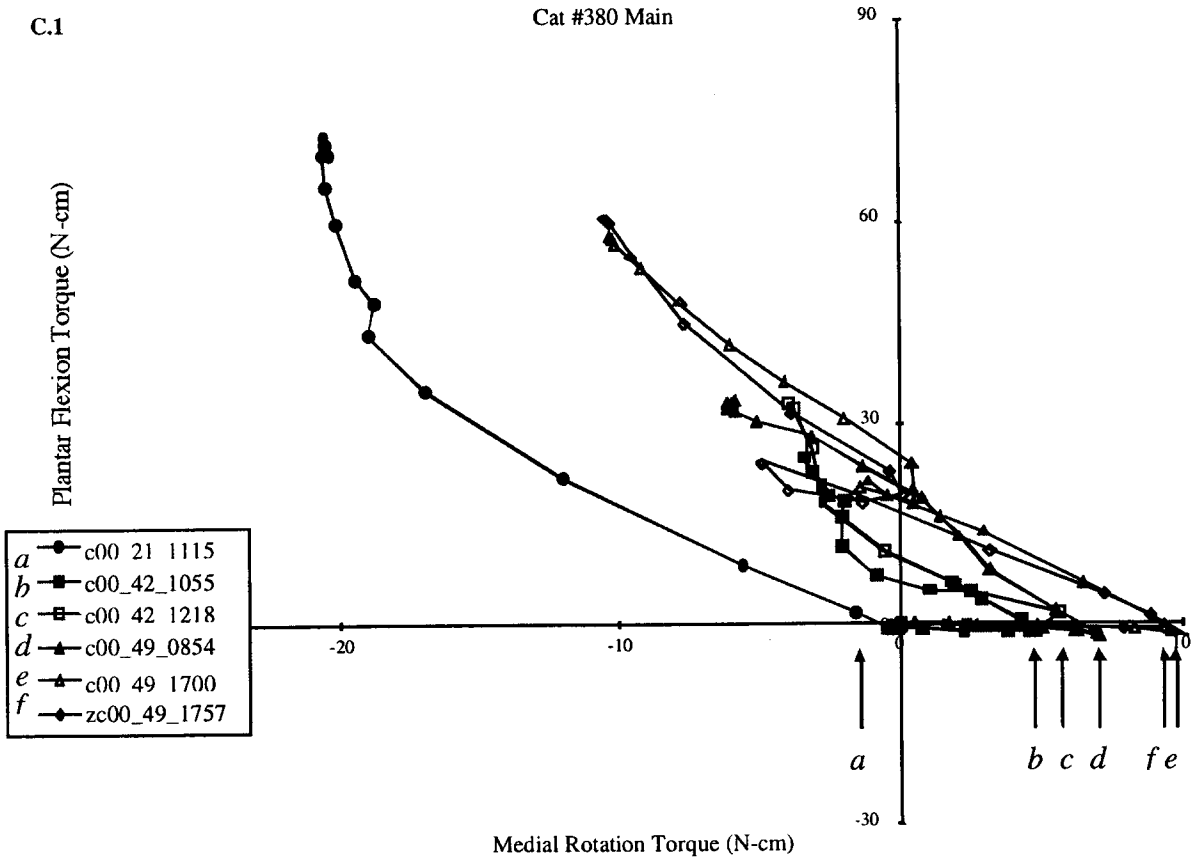

Figure C.1: The output torque produced by stimulation applied to the 0° contact in cat #380. Each label is composed of the contact position (0° contact = 'c00') followed by the number of days post-implant ('21', '42', or '49') and then the time of stimulation. A 'zc' was referred to in one case to indicate that although the test was on the same day as a previous test, the animal was removed and remounted in the frame. In each case, the maximum amount of medial rotation produced in a particular torque trace was indicated by an arrow labeled with a letter corresponding to the figure legend.

In Figure C.2 are the data from stimulation applied to the 90° position contact. Three of the five cases produced an output of about 25 N-cm of lateral rotation and 80 N-cm of plantar flexion. The other two cases produced an output of about 10 N-cm of lateral rotation and 30 N-cm of plantar flexion. This discrepancy in maximal torque output was not dependent on a particular day or experimental mounting position. The discrepancy was even found to occur between two trials within the same experiment. Fatigue is also ruled out since the latter of the two trials produced the larger torque. The cause of this difference in torque amplitude is not clear.

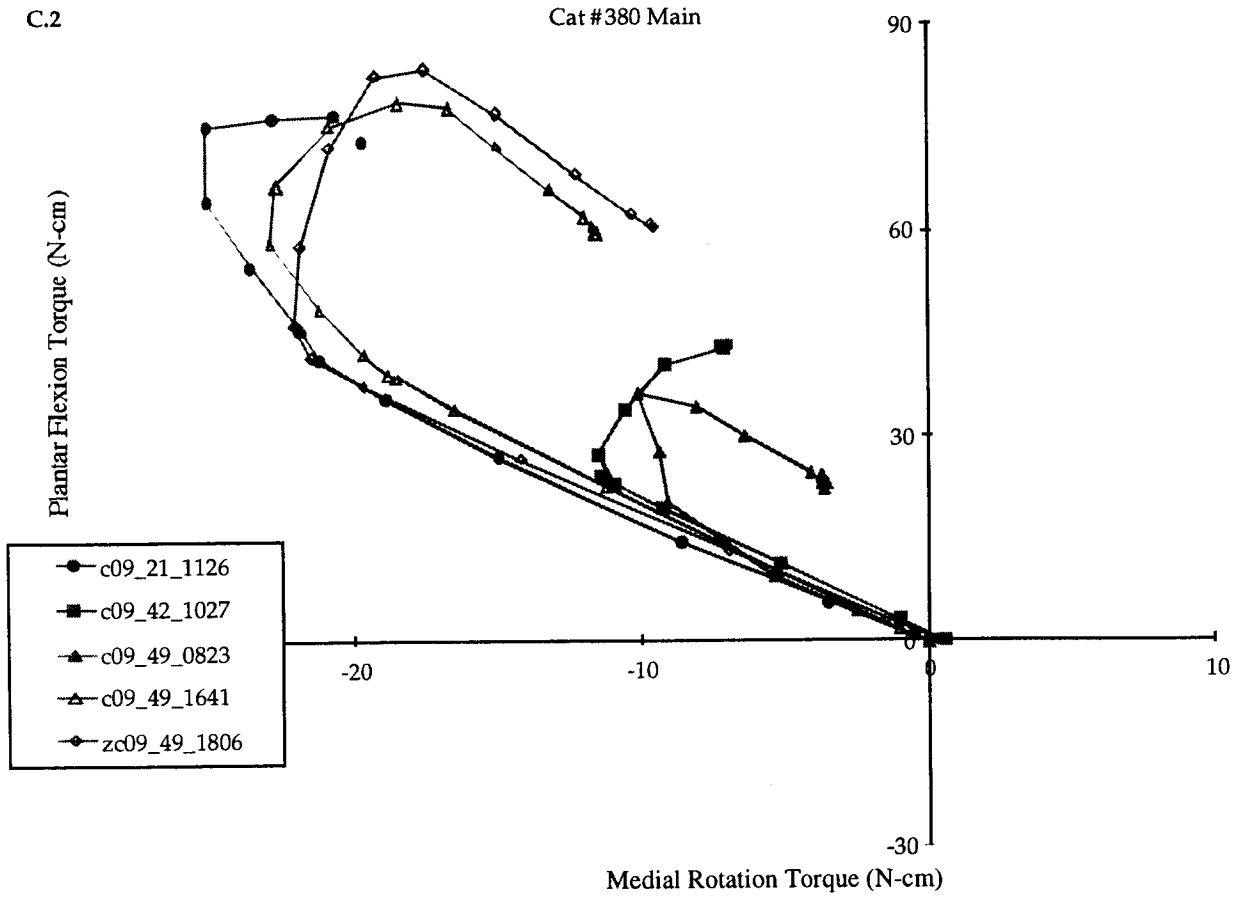

Figure C.2: The output torque produced by stimulation applied to the 90° contact in cat #380. Each label is composed of the contact position (90° contact = 'c09') followed by the number of days post-implant ('21', '42', or '49') and then the time of stimulation. A 'zc' was referred to in one case to indicate that although the test was on the same day as a previous test, the animal was removed and remounted in the frame. In each case, similar direction of output torque was produced. In two cases, the maximum output torque was found to be less that the other three cases.

In Figure C.3 are the data from stimulation applied to the 180° position contact. Although all five torque output traces produce similar directions of output, deviations are

noticeable. Similar to the 90° position, the maximum torque amplitude for an individual curve varied. The maximal torque output varied from 15 N-cm to 25 N-cm of lateral rotation and 40 N-cm to 70 N-cm of plantar flexion. Again, two of the traces performed within the same experiment showed noticeable discrepancy. The latter trial, again, produced a greater torque than the earlier trial.

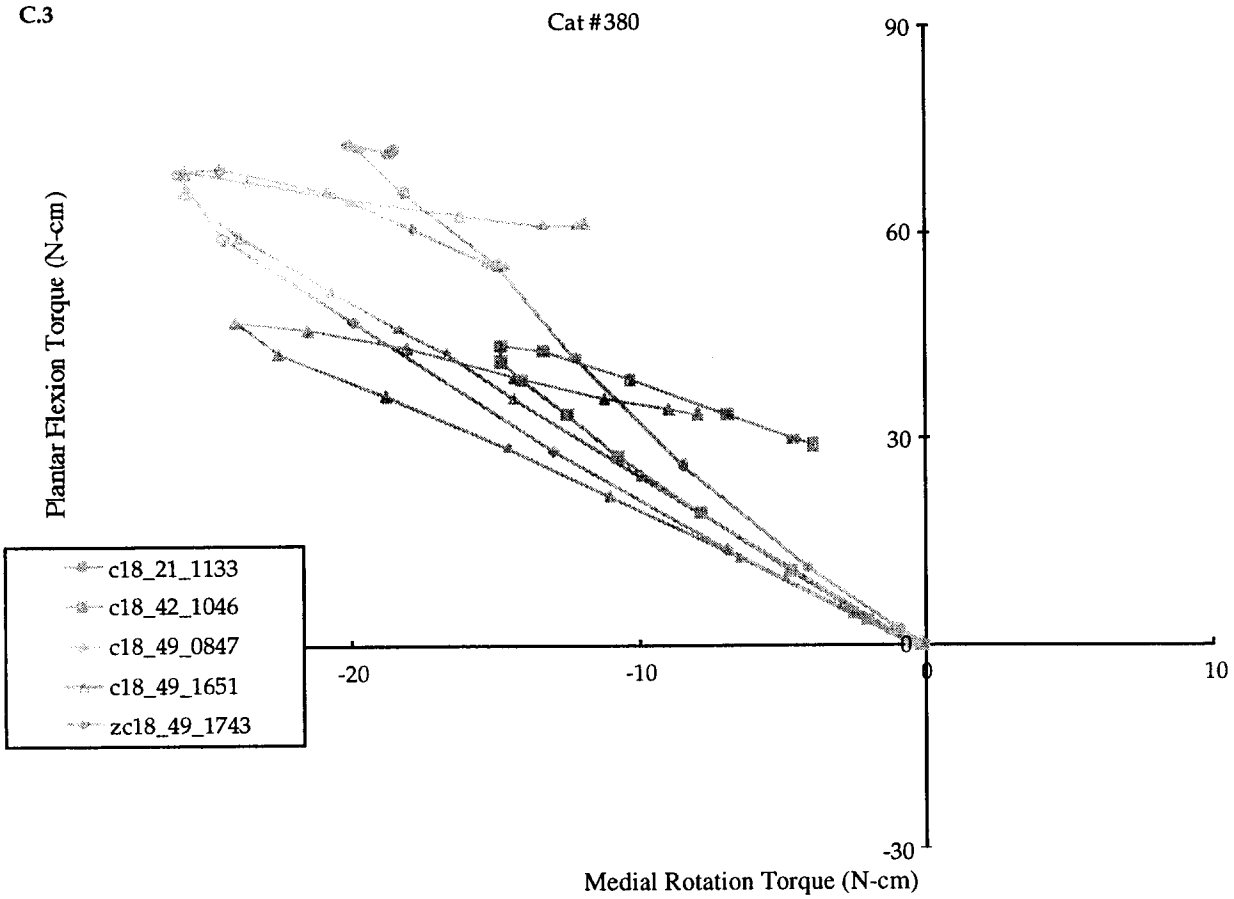

Figure C.3: The output torque produced by stimulation applied to the 180° contact in cat #380. Each label is composed of the contact position (180° contact = 'c18') followed by the number of days post-implant ('21', '42', or '49') and then the time of stimulation. A 'zc' was referred to in one case to indicate that although the test was on the same day as a previous test, the animal was removed and remounted in the frame. In each case, similar direction of output torque was produced but the maximum output torque was found vary.

In Figure C.4 are the data from stimulation applied to the 270° position with anodic steering current from the 180°. Five of the six torque traces produced a combination of dorsi-flexion and medial rotation. The one torque trace that produced plantar flexion with lateral rotation was the only trial that used only partial steering current. In this one trial, c27a(0.9)18s_42_1159, the anodic current passed from the 180° contact to the 270° contact was kept constant at 90% of the determined threshold for that current. Additional monopolar, cathodic current of various amplitudes was applied

between the 270° contact and a distant anode. In the five other torque traces, all of the current was passed between the 180° and 270° contacts. Of these five traces that used complete steering current, only the torque trace from the first experimental day, was found to show a slight deviation from the rest of the torque traces.

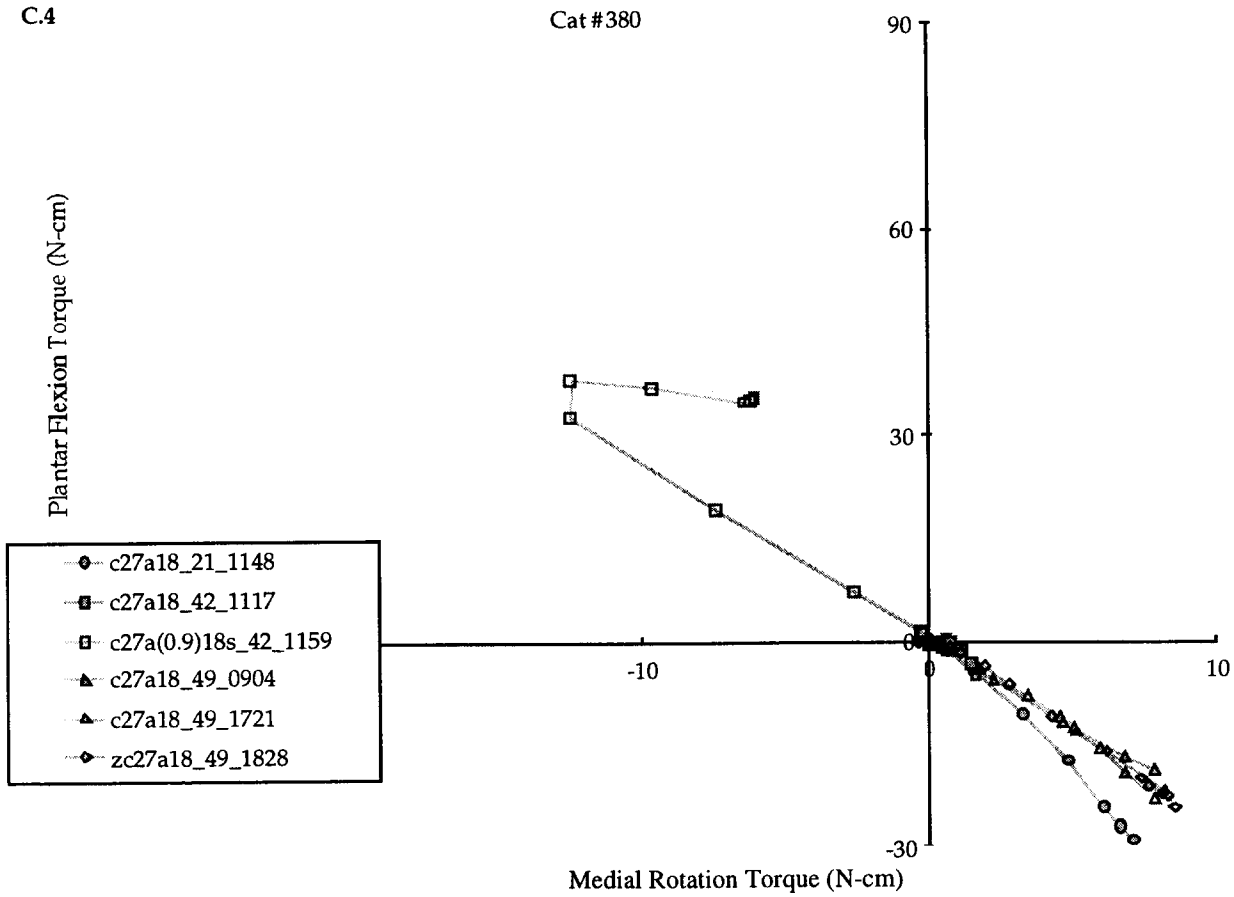

Figure C.4: The output torque produced by stimulation applied to the 270° contact with an anode at the 180° position in cat #380. Each label is composed of the contact position (270° contact with an anode at 180°= 'c27a18') followed by the number of days post-implant ('21', '42', or '49') and then the time of stimulation. A 'zc' was referred to in one case to indicate that although the test was on the same day as a previous test, the animal was removed and remounted in the frame. In 5 of the 6 cases, all of the current was passed between the 270° and the 180° contacts and a similar direction of output torque were produced. The one case that produce plantar flexion torque used a steering configuration where the current was passed between the 270° and 180° contacts was kept at 90% of threshold. The current was then varied between the 270° contact and a distant anode.

The general direction of torque produced by each contact position was consistent through multiple experiments. Variations in the maximal torque amplitudes were

observed in some cases. These variations, however, did not appear to be correlated with time, experimental set-up or fatigue. Future studies will be directed towards gaining an understanding of the reasons for the variability.

C.I.2.3: Continuous torque space

Abstract

The objective of this project is to develop methodologies, suitable for use with cuff electrodes, to effect contraction of multiple muscles, at different levels of activation, to produce any torque output in the physiological torque space. Activation of multiple muscles can be achieved using a field steering approach to shift the activated region between different muscles. Multiple muscle activation can also be achieved by using two different contacts stimulated with a short delay between the pulses to avoid field effects from the combination of pulses. The delay must be long enough to allow partially depolarized axons to return to their resting state but short enough to stay within the refractory period of the axons that were fully depolarized. Previous work established a delay of 900μs as the standard that will be used between two independent stimulation pulses. Stimulation was applied to two different contacts in one animal in an attempt to achieve a range of torque output that was representative of the entire physiological range. The torque output produced by the combined stimulation of two different contacts produced a well sampled area comparable to the area determined by the sum of the vectors produced by single contact stimulation.

Progress

A foreseeable usage for nerve cuff electrodes is for the user (patient, engineer or doctor) to desire a particular torque output. The desired torque output should be produced with minimal co-contraction. Although the problem is still under-constrained, one method for producing the desired torque without a memory intensive look-up table or a complicated neural network has been investigated. Using stimulation from two different contacts that produce activation of different nerve fibers can be used together to produce a range of torque outputs. It was established that a delay of 900μs could be used for independent stimulation. The use of a 900μs delay between two different runs will produce stimulation of all the nerve fibers normally activated by each of the individual runs without the either adding new fibers or stimulating the same fibers twice. Delays of shorter lengths may excite fibers that were slightly depolarized by each pulse but not stimulated by either pulse alone. Delays of longer times can produce stimulation of some of the same fibers twice, once for each stimulation, producing an output for a particular muscle greater than either stimulation would produce alone.

The use of a combination of stimulation from two different contacts was demonstrated in one animal. Figure C.5 contains the torque output vectors produced by each of the contacts alone and in one case the output of two contacts used in a steering configuration. A vector line representing the torque output of each torque trace before spilling over to another fascicle was superimposed on the graph. Using a summation of each of the torque vector lines, a region of space was outlined and define as the functional output region. In Figure C.6 the torque output points produced by various levels of stimulation to a combination of two contacts or one contact and a pair of contacts being stimulated in a steering configuration is shown. The level of stimulation in each case was restricted to be less than the level of stimulation that was deemed to produce an output with spill-over. The functional output region from Figure C.5 is also

superimposed onto the graph in Figure C.6. Within a range of tolerance, the entire region of functional output defined in Figure C.5 was achieved using stimulation from two contacts as shown in Figure C.6. The regions of the defined area of functional output that were not as well sampled were at areas of greater plantar flexion. Some areas outside of the defined functional output range were sampled at greater dorsi-flexion. Neither of these observations appears to be of significant amplitudes.

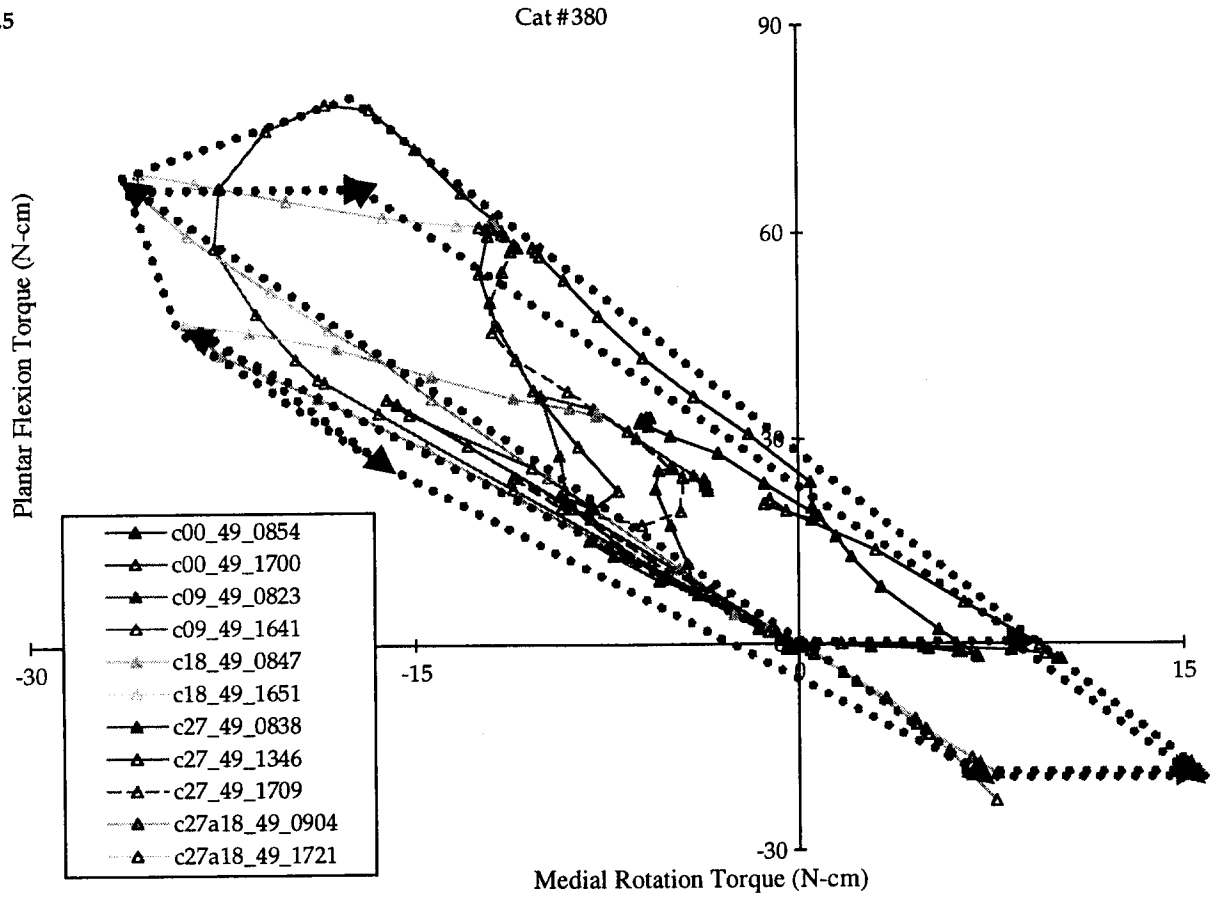

Figure C.5: The output torque produced by stimulation applied to the each contact with in cat #380. Each label is composed of the contact position ('c00'=0°, 'c09'=90°, etc.) followed by the number of days post-implant ('21', '42', or '49') and then the time of stimulation. Superimposed on this figure are individual vectors that have been added together to make a functional torque space that this animal can produce. Each individual vector is found from a single curve that is believed to activate a single fascicle.

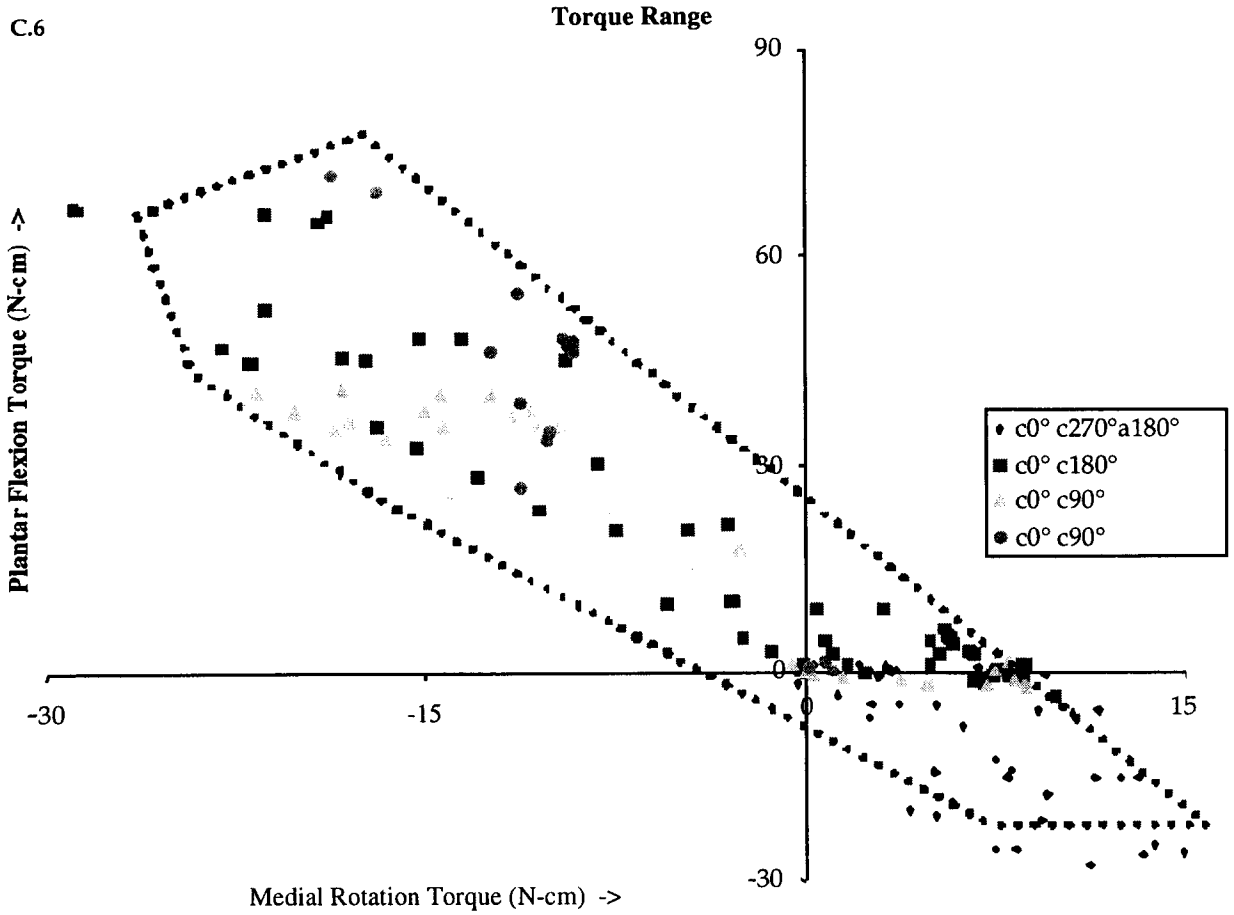

Figure C.6: The output torque produced by stimulation applied to the combinations of contacts with in cat #380. Superimposed on this figure is the functional torque space for this animal that was found in Figure C.5. The torque output produced by the combined stimulation of two different contacts, sub-spillover, was found to fill the functional torque space.